

Negative refraction in Weyl semimetals

M. Shoufie Ukhtary,* Ahmad R. T. Nugraha, and Riichiro Saito
Department of Physics, Tohoku University, Sendai 980-8578, Japan
 (Dated: April 18, 2022)

We theoretically propose that Weyl semimetals may exhibit negative refraction at some frequencies close to the plasmon frequency, allowing electromagnetic waves with frequencies smaller than the plasmon frequency to propagate through the Weyl semimetals. The idea is justified by the calculation of reflection spectra, in which negative (not positive) refractive index at such frequencies give physically correct spectra. In this case, when entering a Weyl semimetal, an electromagnetic wave incident to the surface of the Weyl semimetal will be bent with a negative angle of refraction. We argue that the negative refractive index at the specified frequencies of the electromagnetic wave is required to conserve the energy of the wave, in which the incident energy should propagate away from the point of incidence.

Negative refraction phenomenon has attracted many interests since its prediction by Veselago a half century ago. [1] Veselago predicted that if a material possesses simultaneous negative dielectric constant (ε) and magnetic permeability (μ), it will give a negative refractive index. The negative refractive index will lead to some unusual properties of the light, such as negative refraction and reversed Doppler and Cherenkov effects. [1–4] By utilizing negative refraction, in which the light will be bent in an unusual way with an angle of refraction negative to the normal direction of the material surface, one may be able to construct a superlens whose resolution is smaller than the light wave length. [2–4] A better Cherenkov radiation detector can also be realized based on the material having a negative refractive index, which is useful in the field of accelerator physics. [5, 6] However, materials having simultaneous negative ε and μ have not been found in nature so far.

To realize negative refraction, many researchers developed artificial structures that are called as metamaterials. These structures usually contain an array of split ring resonators [4, 7] or dielectric photonic crystals with periodically modulated ε and μ , [2, 4] which are often complicated to fabricate. To overcome the difficulties, it was predicted that gyrotropic materials, such as chiral media and normal metals in magnetic fields, can exhibit a negative refractive index although μ is positive. [8, 9] In the spirit of this prediction, here we propose that a Weyl semimetal (WSM), whose electric displacement vector is of gyrotropic form even without magnetic field, may have a negative refractive index.

The WSM is a three-dimensional material having at least a pair of separated Dirac cones in its energy dispersion shown in Fig. 1(a). [10–12] An example of the WSM is pyrochlore ($\text{Eu}_2\text{Ir}_2\text{O}_7$). [10, 13] In each cone, the valence and conduction bands coincide at the so-called Weyl nodes. The presence of a pair of separated Dirac cones is the consequence of symmetry breaking in the WSM, which induces the Hall current, even without

magnetic field. [10–12] This phenomenon is known as the anomalous Hall effect, which is responsible for the gyrotropic form of the electric displacement vector of the WSM. [10, 14] We predict that the EM wave can propagate through WSM even though the frequency is smaller than plasmon frequency. This propagation requires the refractive index of WSM to be negative in order to conserve the energy, that will be shown in this letter.

Following some earlier works, [10, 12, 14, 15] the electromagnetic response of a WSM is described by the electric displacement vector \mathbf{D} , which can be written as

$$\mathbf{D} = \varepsilon_0 \varepsilon_b \left(1 - \frac{\omega_p^2}{\omega^2} \right) \mathbf{E} + \frac{ie^2}{4\pi^2 \hbar \omega} \left(2\nabla (\mathbf{b} \cdot \mathbf{r}) \times \mathbf{E} \right), \quad (1)$$

where ω_p is the plasmon frequency, ε_b is the background dielectric constant, and \mathbf{b} is a wave vector separating the Weyl nodes [see Figure 1(a)]. Hereafter, we consider a particular value of the dielectric constant, $\varepsilon_b = 13$, which was measured in pyrochlore. [10, 13] The first term of Eq. (1) is the Drude dielectric function, which is similar to normal metals (NMs). The \mathbf{D} of the WSM is analogous with the case of NMs inside external magnetic fields where the Hall term given by the second term of Eq. (1) corresponds to the anomalous Hall effect due to the symmetry breaking in WSM. Due to the Hall effect, the dielectric tensor has off diagonal terms, which can be written as

$$\varepsilon = \begin{bmatrix} \varepsilon_1 & 0 & i\varepsilon_2 \\ 0 & \varepsilon_1 & 0 \\ -i\varepsilon_2 & 0 & \varepsilon_1 \end{bmatrix} \quad (2)$$

where we assume that $\mathbf{b} = b\hat{\mathbf{y}}$, and that ε_1 and ε_2 are expressed by

$$\varepsilon_1 = \varepsilon_0 \varepsilon_b \left(1 - \frac{1}{\Omega^2} \right), \quad (3)$$

$$\varepsilon_2 = \varepsilon_0 \varepsilon_b \left(\frac{\Omega_{k0}}{\Omega} \right), \quad (4)$$

with $\Omega = \omega/\omega_p$ and $\Omega_b = e^2 b / (2\pi^2 \varepsilon_0 \varepsilon_b \hbar \omega_p)$ as dimensionless quantities. We take $\Omega_b = 0.5$ as a fixed parameter throughout this paper. Similar to NMs, in the WSM we have $\varepsilon_1 > 0$ ($\varepsilon < 0$) if $\Omega > 1$ ($\Omega < 1$).

* shoufie@flex.phys.tohoku.ac.jp

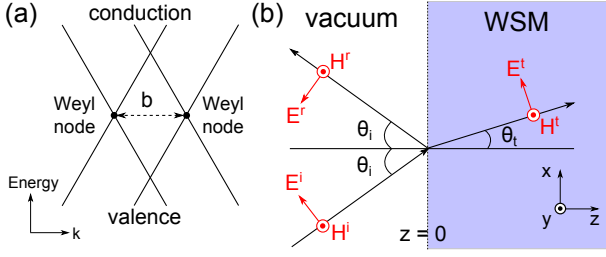


FIG. 1. (a) Schematic energy dispersion of WSM showing a pair of Dirac cones with two Weyl nodes represented by dots, separated by the wave vector b . (b) A TM wave coming to xy surface of WSM (medium 2) at angle θ_i and transmitted to WSM at angle θ_t .

In order to calculate the reflection and transmission spectra of a bulk WSM, we will determine the refractive index (n_w). Suppose we have a transverse magnetic (TM) wave incident at angle θ_i from vacuum to a WSM as shown in Fig. 1(b) where E^i , E^r and E^t (H^i , H^r and H^t) are the incident, reflected and transmitted electric (magnetic) fields, respectively. Due to the vanishing ε_{xy} , the direction of electric field does not rotate. By using Eq. (2), we can write down the equation $\mathbf{D} = \hat{\varepsilon}\mathbf{E}$ for the

TM wave inside the WSM as follows,

$$\begin{bmatrix} D_x^w \\ D_y^w \\ D_z^w \end{bmatrix} = \begin{bmatrix} \varepsilon_1 & 0 & i\varepsilon_2 \\ 0 & \varepsilon_1 & 0 \\ -i\varepsilon_2 & 0 & \varepsilon_1 \end{bmatrix} \begin{bmatrix} E_x^w \\ 0 \\ E_z^w \end{bmatrix} \quad (5)$$

where D^w and E^w are the displacement and electric fields inside the WSM. From Maxwell's equations, we get a differential equation describing an EM wave.

$$\nabla \times \nabla \times \mathbf{E}^w = -\nabla^2 \mathbf{E}^w \nabla (\nabla \cdot \mathbf{E}^w) = \omega^2 \mu_0 \mathbf{D}^w. \quad (6)$$

Since the solutions of \mathbf{E}^w and \mathbf{D}^w are proportional to $\exp[i\omega n_w/c (\mathbf{s} \cdot \mathbf{r})]$, where $\mathbf{s} = (\sin \theta_t, 0, \cos \theta_t)$ is the unit wave vector, we can obtain an equation,

$$\frac{1}{\mu_0} \left(\frac{n_w}{c} \right) [\mathbf{E}^w - \mathbf{s}(\mathbf{s} \cdot \mathbf{E}^w)] = \mathbf{D}^w. \quad (7)$$

From Eqs. (5) and (7), we get

$$E_x^w = \frac{\varepsilon_1 D_x^w - i\varepsilon_2 D_z^w}{\varepsilon_1^2 - \varepsilon_2^2}, \quad \text{and} \quad E_z^w = \frac{i\varepsilon_2 D_x^w + \varepsilon_1 D_z^w}{\varepsilon_1^2 - \varepsilon_2^2}. \quad (8)$$

Inserting Eq. (8) to Eq. (7), we obtain simultaneous equations of E_x^w and E_z^w as follows:

$$\begin{bmatrix} (1 - s_x^2)\varepsilon_1 - i s_x s_z \varepsilon_2 - \mu_0 \left(\frac{c}{n_w} \right)^2 (\varepsilon_1^2 - \varepsilon_2^2) & -i(1 - s_x^2)\varepsilon_2 - s_x s_z \varepsilon_1 \\ i(1 - s_z^2)\varepsilon_2 - s_x s_z \varepsilon_1 & (1 - s_z^2)\varepsilon_1 + i s_x s_z \varepsilon_2 - \mu_0 \left(\frac{c}{n_w} \right)^2 (\varepsilon_1^2 - \varepsilon_2^2) \end{bmatrix} \begin{bmatrix} E_x^w \\ E_z^w \end{bmatrix} \quad (9)$$

To have nontrivial solutions of \mathbf{E}^w , the determinant of the 2×2 matrix in Eq. (9) should vanish:

$$\frac{\mu_0 c^2 (\varepsilon_1^2 - \varepsilon_2^2)}{n_w^4} [-n_w^2 \varepsilon_1 + c^2 \mu_0 (\varepsilon_1^2 - \varepsilon_2^2)] = 0. \quad (10)$$

from which, we obtain n_w ,

$$n_w = \pm c \sqrt{\mu_0 (\varepsilon_1^2 - \varepsilon_2^2) / \varepsilon_1} = n_w^\pm, \quad (11)$$

where the n_w^+ (n_w^-) solution corresponds to the positive (negative) wave vector inside WSM. If we put $\varepsilon_2 = 0$ in Eq. (11), we will recover the refractive index of NM.

In Fig. 2(a) we plot n_w as a function of Ω for the positive solution of Eq. (11) (n_w^+). The solid and the dashed lines correspond to the real and imaginary parts of n_w^+ , respectively. It is noted that n_w^+ at each frequency is either purely real or purely imaginary, because we ignore the impurity and scattering of charge in Eq. (3). Therefore, the wave vector $\omega n_w^+ / c$ can be either real or imaginary depending on n_w^+ . The real (imaginary) wave vector represents a propagating (decaying) wave.

Here we divide our results into four regions as shown in Fig. 2(a): region I ($0 \leq \Omega \leq \Omega_-$), region II

($\Omega_- \leq \Omega \leq 1$), region III ($1 \leq \Omega \leq \Omega_+$) and region

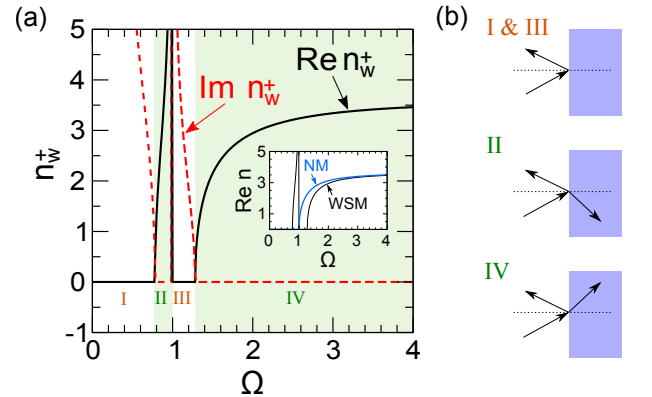


FIG. 2. (a) The refractive index of WSM for TM wave (n_w) as a function of Ω . Solid and dashed lines are the real and imaginary parts of n_w^+ , respectively. We use $\Omega_b = 0.5$ for the WSM. The plot is divided into four regions. Inset: The real part of refractive index (n) for the WSM compared with a normal metal (NM). All plots are the positive solutions of Eq. (11). (b) Schematics of EM wave propagations to the WSM for all the four regions of panel (a).

IV ($\Omega_+ \leq \Omega$), where $\Omega_{\pm} = 1/2 \left(\pm\Omega_b + \sqrt{4 + \Omega_b^2} \right)$ are frequencies that give $n_w = 0$ [Eqs. (3), (4), (11)]. If we use $\Omega_b = 0.5$ and $\omega_p = 9$ THz measured in pyrochlore for $E_F = 8.62$ eV, [10, 13] the corresponding regions are ($0 \leq \omega \leq 7.03$ THz) for region I, ($7.03 \leq \omega \leq 9$ THz) for region II, ($9 \leq \omega \leq 11.8$ THz) for region III and (11.8 THz $\leq \omega$) for region IV.

From Fig. 2(a), we can see that we may have a propagating wave even at frequencies smaller than plasmon frequency ($\Omega < 1$), indicated by the shaded region II, which is in contrast with NM where an EM wave can propagate if $\Omega > 1$ [see inset of Fig. 2(a)]. The refractive indices of WSM and NM differ only at $\Omega \simeq 1$. At $\Omega \gg 1$, they both converge to the value of $n \approx \sqrt{\varepsilon_b}$. It is important to note that the negative solution of Eq. (11) (n_w^-) is needed to have propagating wave at $\Omega < 1$, which will be shown later. With this information, the reflection and transmission spectra can now be calculated.

Following the schematics in Fig. 1(b), the electric fields \mathbf{E}_i , \mathbf{E}_r and \mathbf{E}_t can be written as

$$\mathbf{E}^i(z) = (\cos \theta_i, 0, -\sin \theta_i) E_0^i \exp(ik_{vz}z), \quad (12)$$

$$\mathbf{E}^r(z) = (-\cos \theta_i, 0, -\sin \theta_i) E_0^r \exp(-ik_{vz}z), \quad (13)$$

$$\mathbf{E}^t(z) = (\cos \theta_t, 0, -\sin \theta_t) E_0^t \exp(ik_{wz}^{\pm}z), \quad (14)$$

with $k_{vz} = (\omega/c) \cos \theta_i$ and $k_{wz}^{\pm} = \omega(n_w^{\pm}/c) \cos \theta_t$. The angles θ_i and θ_t are related through Snell's law $\sin \theta_i = n_w^{\pm} \sin \theta_t$. The magnetic fields in y direction can be obtained from the relations $H_y^{i,r} = i\omega \int \varepsilon_0 E_x^{i,r} dz$ and $H_y^t = i\omega \int D_x^w dz$, where $D_x^w = \varepsilon_1 E_x^w + i\varepsilon_2 E_z^w$ is obtained from Eq. (5). The magnetic fields can be written as

$$\mathbf{H}^i(z) = \frac{\omega \varepsilon_0}{k_{az}} (0, \cos \theta_i, 0) E_0^i \exp(ik_{vz}z), \quad (15)$$

$$\mathbf{H}^r(z) = \frac{\omega \varepsilon_0}{k_{vz}} (0, \cos \theta_i, 0) E_0^r \exp(-ik_{vz}z), \quad (16)$$

$$\mathbf{H}^t(z) = \frac{\omega}{k_{wz}} (0, \varepsilon_1 \cos \theta_t - i\varepsilon_2 \sin \theta_t, 0) E_0^t \times \exp(ik_{wz}^{\pm}z). \quad (17)$$

After defining the EM fields in both media, we can write down the boundary conditions of EM wave on incidence surface ($z = 0$) as follows,

$$E_0^i \cos \theta_i - E_0^r \cos \theta_i = E_0^t \cos \theta_t, \quad (18)$$

and

$$\begin{aligned} & \frac{\omega \varepsilon_0}{k_{vz}} (E_0^i \cos \theta_i + E_0^r \cos \theta_i) \\ &= \frac{\omega}{k_{wz}^{\pm}} (\varepsilon_1 E_0^t \cos \theta_t - i\varepsilon_2 E_0^t \sin \theta_t), \end{aligned} \quad (19)$$

where Eqs. (18) and (19) describe the continuity of electric fields and magnetic fields at $z = 0$, respectively. Reflection coefficient $r = E_0^r/E_0^i$ and transmission coefficient $t = E_0^t/E_0^i$ are defined by

$$r = 1 - t \frac{\cos \theta_t}{\cos \theta_i}, \quad (20)$$

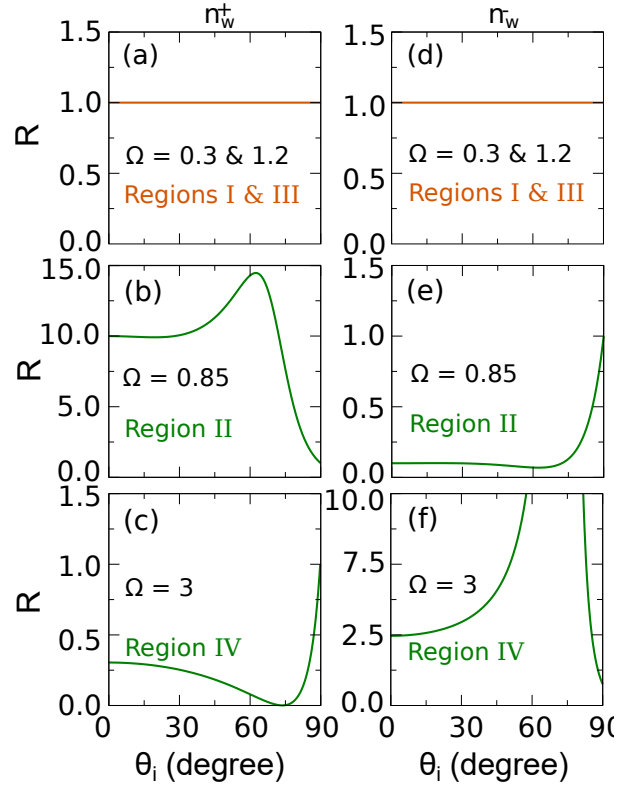


FIG. 3. The reflection probability (R) of the EM wave in a WSM for (a) regions I [$\Omega = 0.3$] and III [$\Omega = 1.2$], (b) region III [$\Omega = 0.85$] and (c) region IV [$\Omega = 3$] if we use n_w^+ . Panels (d)–(f) show the corresponding R spectra if we use n_w^- . The negative solution gives physically correct spectra, i.e., $R \leq 1$ in region II [panel (e)], while in the other regions, positive solutions should be used.

and

$$t = \frac{2k_{wz}^{\pm} \varepsilon_0 \cos \theta_i}{k_{vz} (\varepsilon_1 \cos \theta_t - i\varepsilon_2 \sin \theta_t) + k_{wz}^{\pm} \varepsilon_0 \cos \theta_t}. \quad (21)$$

In Fig. 3, we plot the reflection probability defined by $R = |r|^2$ as a function of θ_i . In region I and III the incident EM wave will be totally reflected $R = 1$ for all θ_i for both n_w^{\pm} as shown in Fig. 3(a) and (d), due to the purely imaginary n_w^{\pm} given in Fig. 2(a). The \mathbf{E}^t is decaying inside WSM, hence no transmitted energy into WSM. The most interesting case is region II, where we predict that WSM acquires a negative refractive index. In region II, we have a real n_w^{\pm} , which means that the wave propagation inside WSM is allowed, even though the wave frequency is smaller than the plasmon frequency. In Figs. 3(b) and 3(e), we plot R as a function of θ_i for both n_w^+ and n_w^- , respectively.

Normally, we use n_w^+ which gives a positive value of k_{wz}^{\pm} because the transmitted wave propagates to positive z direction [see Eq. (14)]. However, n_w^+ for the transmitted wave gives an unphysical $R > 1$ shown by Fig. 3(b), which means that at the point of incidence there is a flux of energy coming from the WSM side. At the point of

incidence, the source of energy is only the incident EM wave; and due to the energy conservation, the energy should propagate away from the point toward negative z direction as reflected wave and toward positive z direction as transmitted wave. The problem is overcome by adopting n_w^- , from which we get a physically sound $R \leq 1$ as shown in Fig. 3(e). This negative solution (n_w^-) should be selected only for region II, because if we apply n_w^- to region IV, we have an unphysical $R > 1$ given by Fig. 3(f). In region IV, the WSM acts as a NM for $\Omega > 1$. Figure 3(c) shows $R = 0$ at $\theta_i = \arctan n_w$, which corresponds to the Brewster angle.

The negative refractive index of WSM in region II will cause the wave refracted negatively, which means that the refracted angle θ_t is negative. The refractive index also means that the wave vector of transmitted wave (k_{wz}^-) is negative, i.e. the direction of wave vector is toward the point of incidence. The negative wave vector does not mean that the transmitted wave propagates toward the point of incident, which violates the conservation of energy explained before. The direction of propagation can be different with the wave vector in anisotropic media and anti parallel in metamaterial having negative refractive index. [16–19] The direction of propagation can be determined by the direction of the Poynting vector where at the point of incidence, the net power transmitted in the direction of z can be expressed as

$$\begin{aligned} I_t &= \frac{1}{2} \text{Re} \left[\mathbf{E}^t(0) \times \mathbf{H}^{*t}(0) \right] \cdot \hat{\mathbf{z}} \\ &= \frac{c|t|^2 |E_0^i|^2}{2n_w^\pm} \varepsilon_1 \cos \theta_t, \end{aligned} \quad (22)$$

where we use Eqs. (14) and (17) to calculate Eq. (22). In order to have transmitted power propagate in positive z direction, Eq. (22) should have a positive value. Since $\varepsilon_1 < 0$ in region II [Eq. (3)], while $|t|^2$, $|E_0^i|^2$, and $\cos \theta_t > 0$, n_w^\pm has to be negative (n_w^-) in order to have $I_t > 0$. On the other hand, n_w^+ is selected in region IV, because $\varepsilon_1 > 1$.

Using Eq. (22), the transmission probability T is defined as

$$T = \frac{I_t}{I_i} = \frac{1}{\varepsilon_0} \frac{\varepsilon_1 \cos \theta_t}{n_w^\pm \cos \theta_i} |t|^2, \quad (23)$$

where $I_i = (c/2) |E_0^i|^2 \varepsilon_0 \cos \theta_i$ is the incident intensity. The reflection probability R is given by $R = 1 - T$. In Figs. 4(a) and 4(b) we show the R and T spectra for region II ($\Omega = 0.85$) and region IV ($\Omega = 3$), where the EM wave propagation is allowed. In the case of region II, we adopt the n_w^- , while in the case of region IV, we adopt n_w^+ . In Fig. 4(c), we plot the R and T spectra as a function of Ω at a fixed incident angle $\theta_i = 20^\circ$. In region II, we expect that the negative refraction can take place. In NM, all EM wave is reflected in this region due to the imaginary transmitted wave vector. In region II, the R gradually decreases as a function of Ω because

the transmitted wave vector acquires real value, which signifies the transmission of the incident wave to WSM. After reaching the minimum, the reflection probability increases gradually up to $R = 1$, where the transmitted wave vector acquires imaginary value that makes $T = 0$. The negative refraction in WSM occurs in region II where the frequencies are close to ω_p , which can be seen in Fig. 4(c). This result is consistent with the previous prediction of negative refraction in gyrotropic media, in which the frequencies close to ω_p is important for having negative refraction. [8]

In conclusion, we have shown theoretically that negative refraction can occur in the WSM, which is justified from its reflection spectra. The refractive index of WSM is negative at a specific frequency range close to the plasmon frequency, suggesting the WSM as a kind of gyrotropic media. The negative refractive index is required for the propagation of the EM wave with frequency smaller than the plasmon frequency to uphold the conservation of energy. We suggest that by using only the WSM it is not necessary to make a complicated structure of metamaterials to obtain negative refraction. It would be desired if the phenomenon could be measured in future experiments, especially for much larger plasmon frequencies.

M.S.U is supported by the MEXT scholarship, Japan. A.R.T.N. acknowledges the Leading Graduate School in Tohoku University. R.S. acknowledges JSPS KAKENHI Grant Numbers JP25107005 and JP25286005.

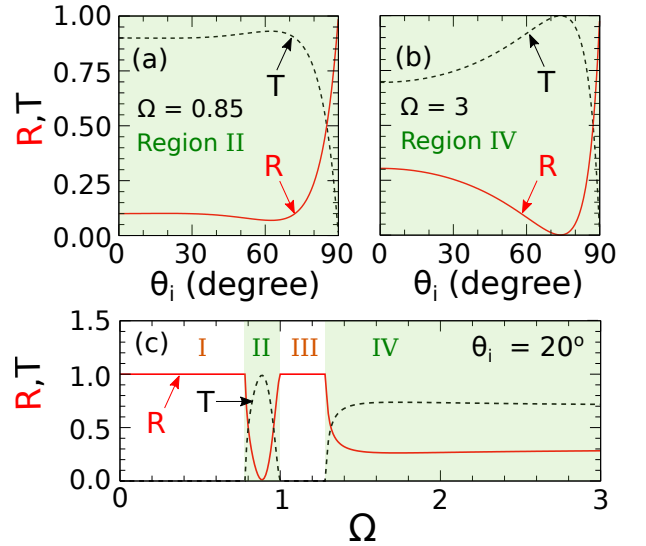


FIG. 4. The R and T spectra as a function of θ_i shown as solid and dashed line, respectively, for (a) region II ($\Omega = 0.85$), (b) region IV ($\Omega = 3$). In (a) the negative solution of n_w is used, while in (b) the positive one is used. In both cases, $R + T = 1$. (c) The R and T spectra as a function of Ω with fixed $\theta_i = 20^\circ$ shown as solid and dashed line, respectively. In shaded regions II and IV, the wave is transmitted. However, only in region II we expect that negative refraction could occur.

-
- [1] V. G. Veselago, Phys. Usp. **10**, 509 (1968).
- [2] E. Cubukcu, K. Aydin, E. Ozbay, S. Foteinopoulou, and C. M. Soukoulis, Nature **423**, 604 (2003).
- [3] J. B. Pendry, Phys. Rev. Lett. **85**, 3966 (2000).
- [4] D. R. Smith, J. B. Pendry, and M. C. K. Wiltshire, Science **305**, 788 (2004).
- [5] J. Lu, T. M. Grzegorzczak, Y. Zhang, J. Pacheco Jr, B.-I. Wu, J. A. Kong, and M. Chen, Opt. Express **11**, 723 (2003).
- [6] D. Ziemkiewicz and S. Zielińska-Raczyńska, J. Opt. Soc. Am. B **32**, 1637 (2015).
- [7] A. Ishikawa, T. Tanaka, and S. Kawata, Physical review letters **95**, 237401 (2005).
- [8] V. M. Agranovich, Y. N. Gartstein, and A. A. Zakhidov, Phys. Rev. B **73**, 045114 (2006).
- [9] J. B. Pendry, Science **306**, 1353 (2004).
- [10] J. Hofmann and S. Das Sarma, Phys. Rev. B **93**, 241402 (2016).
- [11] A. A. Burkov and L. Balents, Phys. Rev. Lett. **107**, 127205 (2011).
- [12] M. M. Vazifeh and M. Franz, Phys. Rev. Lett. **111**, 027201 (2013).
- [13] A. B. Sushkov, J. B. Hofmann, G. S. Jenkins, J. Ishikawa, S. Nakatsuji, S. Das Sarma, and H. D. Drew, Phys. Rev. B **92**, 241108 (2015).
- [14] A. A. Zyuzin and V. A. Zyuzin, Phys. Rev. B **92**, 115310 (2015).
- [15] A. G. Grushin, Phys. Rev. D **86**, 045001 (2012).
- [16] B. E. A. Saleh and M. C. Teich, *Fundamentals of photonics* (Wiley, New York, 1991).
- [17] D. R. Smith and N. Kroll, Phys. Rev. Lett. **85**, 2933 (2000).
- [18] S. A. Ramakrishna, Rep. Prog. Phys. **68**, 449 (2005).
- [19] J. Woodley and M. Mojahedi, J. Opt. Soc. Am. B **23**, 2377 (2006).